Title

A comparison between Gauss-Newton and Markov chain Monte Carlo based methods for inverting spectral induced polarization data for Cole-Cole parameters

Author

Hawkes, Daniel S

Publication Date

2008-11-06

Peer reviewed

A comparison between Gauss-Newton and Markov chain Monte Carlo based methods for inverting spectral induced polarization data for Cole-Cole parameters

Jinsong Chen[1], Andreas Kemna[2] and Susan S. Hubbard[1]

1: Earth Sciences Division, Lawrence Berkeley National Laboratory, USA;

Email: jchen@lbl.gov and sshubbard@lbl.gov

2: formerly: Agrosphere (ICG-4), Forschungszentrum Jülich, 52425 Jülich, Germany;

now at: Department of Geodynamics and Geophysics, University of Bonn, Nussallee 8,

53115 Bonn, Germany;

Email: kemna@geo.uni-bonn.de

ABSTRACT

We develop a Bayesian model to invert spectral induced polarization (SIP) data for Cole-Cole parameters using Markov chain Monte Carlo (MCMC) sampling methods. We compare the performance of the MCMC based stochastic method with an iterative Gauss-Newton based deterministic method for Cole-Cole parameter estimation through inversion of synthetic and laboratory SIP data. The Gauss-Newton based method can provide an optimal solution for given objective functions under constraints, but the obtained optimal solution generally depends on the choice of initial values and the estimated uncertainty information is often inaccurate or insufficient. In contrast, the MCMC based inversion method provides extensive global information on unknown parameters, such as the marginal probability distribution functions, from which we can obtain better estimates and tighter uncertainty bounds of the parameters than with the deterministic method. Additionally, the results obtained with the MCMC method are independent of the choice of initial values. Because the MCMC based method does not explicitly offer single optimal solution for given objective functions, the deterministic and stochastic methods can complement each other. For example, the stochastic method can first be used to obtain the means of the unknown parameters by starting from an arbitrary set of initial values and the deterministic method can then be initiated using the means as starting values to obtain the optimal estimates of the Cole-Cole parameters.

INTRODUCTION

The induced polarization (IP) method has been increasingly used in environmental investigations because IP measurements are very sensitive to the low frequency capacitive properties of rocks and soils. These properties are associated with diffusion-controlled polarization processes that occur at the mineral-fluid interface (Slater and Lesmes, 2002). The Cole-Cole model (Cole and Cole, 1941) has been found to be very useful for interpreting spectral IP (SIP) data in terms of parameters, such as chargeability and time constant, which in turn have been used to estimate various subsurface properties (Lesmes and Friedman, 2005). Among many studies in which Cole-Cole parameters were estimated from SIP measurements on soils and rocks, the majority employed classical deterministic inversion methods, specifically the iterative Gauss-Newton based schemes with the Levenberg-Marquardt damping for stabilization of the inverse solution (Pelton et al., 1984; Jaggar and Fell, 1988; Luo and Zhang, 1998; Kemna, 2000; Boadu and Seabrook, 2000).

Two popular routines have been developed for Cole-Cole parameter estimation according to the iterative Gauss-Newton algorithms. The first, developed by Pelton et al. (1978), has been extensively demonstrated on SIP data from mineralized rock; the second, developed by Kemna (2000), has been widely used for inverting SIP data associated with sediments and calibrated materials (Kemna et al., 2000, 2005; Binley et al., 2005; Slater et al., 2005, 2006; Mansoor and Slater, 2007). Although the two routines are different in terms of parameterization and definition of data, they are common in the use of the derivatives of the forward model with respect to model parameters (i.e., Jacobian matrix) to iteratively update the Cole-Cole parameters from a set of initial values.

The main limitation of the Gauss-Newton based deterministic method is that the convergence to the global minimum is not guaranteed and the estimation results strongly depend on the choice of the starting values. Consequently, successful application of the deterministic method for SIP data inversion requires considerable familiarity with the characteristics of Cole-Cole model responses and with the sensitivity to the underlying Cole-Cole parameters. A multiple Cole-Cole model is typically used for describing the SIP responses where multiple relaxation mechanisms are superimposed. In such cases, it is often difficult to choose suitable sets of initial values in order to obtain an optimal solution of the Cole-Cole parameters.

Other types of inversion approaches have also been suggested to reduce the dependence of the optimal solution on the initial values. Examples include a direct scheme by Xiang et al. (2001), which consists of a multifold least-squares estimation combined with an optimal searching technique, a genetic algorithm by Cao et al. (2005), and a robust Gauss-Newton based method with adaptive regularization by Roy (1999). The main disadvantage of those methods is that they provide inaccurate or insufficient information on uncertainty in the parameter estimation.

Ghorbani et al. (2007) developed a Bayesian model to invert time and frequency domain IP data for parameters in a single Cole-Cole model. They used a numerical integration technique over regular grids to obtain a marginal posterior probability density function (pdf) of each Cole-Cole parameter from the joint posterior probability distribution function. Through case studies based on synthetic and laboratory data sets, they demonstrated that the Bayesian model could provide the estimates of the marginal probability density function of each unknown parameter and of each paired unknown parameters. However, their method for obtaining many samples from the joint posterior distribution is very difficult to apply in practice because of the high dimensionality of the unknown parameter space, which commonly occurs with a multiple Cole-Cole model. As described in next section, a multiple Cole-Cole model is a more general and proper model than a single Cole-Cole model for describing IP data with various dispersion ranges, either due to multiple length scales in sediments or due to the coupling effects in the IP measurements.

We begin with a review of the Cole-Cole model. This is followed by our development of a Bayesian model to invert SIP data for Cole-Cole parameters using Markov chain Monte Carlo (MCMC) sampling methods (Gilks et al., 1996). MCMC methods are effective methods for drawing samples from complex and high-dimensional joint probability distribution functions and have been increasingly used to invert complex geophysical data (Bosch, 1999; Buland and Omre, 2003; Gunning and Glinsky, 2004; Chen et al., 2004, 2006). Our goal is to develop an inversion approach that is insensitive to initial values and that provides sufficient uncertainty information on the estimation when we invert SIP data for parameters in a multiple Cole-Cole model. We evaluate the performance of the sampling-based Bayesian model by applying it to both synthetic and laboratory SIP data sets and comparing the inversion results with those obtained from the Gauss-Newton based deterministic method developed by Kemna (2000).

COLE-COLE MODEL

We interpret spectral induced polarization data using the Cole-Cole model (Cole and Cole, 1941; Pelton et al., 1978), which is an empirical extension of the classic Debye relaxation model. For complex resistivity, describing the electric voltage response to an electric current excitation in the frequency domain, the Cole-Cole model can be written as

$$\rho(\omega) = \rho_0 \left\{ 1 - m \left[1 - \frac{1}{1 + (j\omega\tau)^c} \right] \right\}, \tag{1}$$

where ρ_0 is the asymptotic resistivity value towards zero frequency, m is the chargeability that describes the magnitude of electric polarization giving rise to the phase shift between voltage and current (i.e., the complex nature of ρ), τ is the characteristic time constant of the relaxation process, and c is the Cole-Cole exponent that describes the degree of frequency dependence of ρ. In the equation, ω and j are the angular frequency and $\sqrt{-1}$, respectively. For $c = 1$, the Cole-Cole model is reduced to the Debye model. Table 1 list variables and symbols used in this paper. Note that both Cole-Cole and Debye models are characterized by a single peak in the complex resistivity phase spectrum; the location of the peak along the frequency axis is directly related to the relaxation time constant τ.

The Cole-Cole model was introduced by Pelton et al. (1978) to describe electrical properties in mineralized rock, where polarization occurs at interfaces between electronically conducting mineral grains and fluid-filled pores with electrolytic conduction. Over the last decade, the model has been adopted to describe the observed complex resistivity response of sedimentary rock that does not include electronically conducting components (Vanhala, 1997; Binley et al., 2005; Kemna et al., 2005) and normally exhibits a much weaker phase response than does mineralized rock. In that case, polarization is a result of the interaction of the pore fluid (electrolyte) with electrically charged mineral surfaces, where the so-called electric double layer is formed (e.g., Leroy et al., 2008).

Importantly, for both polarization mechanisms, the observed time scale of relaxation, as quantified by the Cole-Cole time constant τ, is directly related to the length scale determined by the size of electronically conducting grains in mineralized rock (Pelton et al., 1978) or by the length scale characteristic of the pore space in sedimentary rock (e.g., Titov et al., 2002; Scott and Barker, 2003; Binley et al., 2005; Slater, 2007). In this sense, the measured complex resistivity spectrum represents an integrated response over all length scales presented in the rock (e.g., Leroy et al., 2008). For rock with a unimodal distribution of length scales (i.e., a unimodal grain or pore size distribution), a phase spectrum with a single peak, as numerously reported in the literature, can be expected. However, for more complex distributions of length scales, such as bimodal distributions, phase spectra with more than one phase peak can be observed (Leroy et al., 2008). The different peaks reflect relaxation processes at different scales. Such behavior was also observed in time-domain measurements of induced polarization (Tong et al., 2006; Tarasov and Titov, 2007).

An additional frequency dependence in the measured complex resistivity spectrum is typically generated by inductive and/or capacitive coupling effects associated with the instrumentation and cable layout. These can be phenomenologically also described by a Cole-Cole dispersion term (e.g., Pelton et al., 1978; Kemna et al., 1999, 2005). In this case, however, the Cole-Cole parameters themselves are normally not of interest, but only the response of the parameter set with an objective of removing it from the measured data.

We adopt a multiple Cole-Cole model as used by Kemna (2000) to allow for analysis of phase spectra with more than one dispersion range caused either by the multiple modality of the rock or by the coupling effects in the measurements. Such a model represents a discrete integration over different relaxation scales and is given by

$$\rho(\omega) = \rho_0 \left\{ 1 - \sum_{l=1}^{L} m_l \left[1 - \frac{1}{1 + (j\omega\tau_l)^{c_l}} \right] \right\}, \tag{2}$$

where L is the number of Cole-Cole models that we fit for a given complex resistivity data set. A typical value for L is between 1 and 3, depending on the number of present relaxation scales and whether the inversion procedure is applied to remove coupling effects from the measured data or to extract intrinsic Cole-Cole parameters from complex resistivity imaging results

(Kemna et al., 2000). The symbols m_l, τ_l, and c_l represent chargeability, time constant, and dependence factor for the $l-th$ dispersion term of the multiple Cole-Cole model, respectively.

The Cole-Cole model given in equation (2) can be rewritten in the form of real and imaginary components of complex resistivity as given by Cao et al. (2005)

$$\mathrm{Re}[\rho(\omega_k)] = \rho_0 \left[1 - \sum_{l=1}^{L} m_l \left(1 - \frac{R_l}{R_l^2 + I_l^2}\right)\right], \tag{3}$$

$$\mathrm{Im}[\rho(\omega_k)] = -\rho_0 \sum_{l=1}^{L} m_l \frac{I_l}{R_l^2 + I_l^2}, \tag{4}$$

where $\omega_k = 2\pi f_k$, $k = 1, 2, \cdots, n$ (f_k is the $k-th$ frequency and n is the total number of frequencies at which the IP measurements are collected), $R_l = (\omega\tau_l)^{c_l}\cos(c_l\pi/2) + 1$, and $I_l = (\omega\tau_l)^{c_l}\sin(c_l\pi/2)$.

STOCHASTIC METHOD

Bayesian framework

We develop a Bayesian model to estimate parameters in the Cole-Cole model given by equations (3) and (4). The SIP data used for this model are the real and imaginary components (i.e., $\mathrm{Re}[\rho^{obs}(\omega_k)]$ and $\mathrm{Im}[\rho^{obs}(\omega_k)]$) of the complex resistivity collected at frequency ω_k ($k = 1, 2, \cdots, n$), the unknown parameters are the zero-frequency resistivity ρ_0, the base 10 logarithmic chargeability $\mathbf{m} = (\log(m_1),\ \log(m_2),\ \cdots,\ \log(m_L))^T$, the base 10 logarithmic time constant $\mathbf{b} = (\log(\tau_1),\ \log(\tau_2),\ \cdots,\ \log(\tau_L))^T$, and the dependence factor $\mathbf{c} = (c_1, c_2, \cdots, c_L)^T$. To account for the unknown measurement errors in the real and imaginary components, we include two additional parameters u_{re} and u_{im}, which are the inverse variances of the measurement errors in the real and imaginary parts of complex resistivity. As a result, we can write the Bayesian model as

$$\begin{aligned} & f(\rho_0, \mathbf{m}, \mathbf{b}, \mathbf{c}, u_{re}, u_{im} \mid \{\mathrm{Re}[\rho^{obs}(\omega_i)], \mathrm{Im}[\rho^{obs}(\omega_k)],\ k = 1, 2, \cdots, n\}) \\ & \quad \propto \prod_{k=1}^{n} f(\mathrm{Re}[\rho^{obs}(\omega_k)] \mid \rho_0, \mathbf{m}, \mathbf{b}, \mathbf{c}, u_{re}) \\ & \qquad \prod_{i=1}^{n} f(\mathrm{Im}[\rho^{obs}(\omega_k)] \mid \rho_0, \mathbf{m}, \mathbf{b}, \mathbf{c}, u_{im}) \\ & \qquad f(\rho_0, \mathbf{m}, \mathbf{b}, \mathbf{c}, u_{re}, u_{im}). \end{aligned} \tag{5}$$

The first and second terms on the right side of equation (5) are the likelihood functions of the real and imaginary components of complex resistivity data, respectively; the third term is the prior distribution function of unknown Cole-Cole parameters. Because we assume that the real and imaginary parts of complex resistivity at different frequencies are independent of each other, we can write the expression in the form of the product of individual likelihood functions as shown in equation (5). Below we define the likelihood functions and the prior distributions that are included in the equation.

Likelihood functions

To define the likelihood function of the real components of complex resistivity, we assume that the relative errors between the observed data and the output of the forward Cole-Cole model have a normal distribution with zero mean and unknown inverse variance, that is,

$$e_k^r = \frac{\mathrm{Re}[\rho^{obs}(\omega_k)] - \mathrm{Re}[\rho(\omega_k)]}{\mathrm{Re}[\rho^{obs}(\omega_k)]} \sim N(0, u_{re}). \tag{6}$$

We choose this likelihood model partly because errors in IP data often have a distribution close to the normal distribution and partly because the maximum likelihood estimates of such types of likelihood functions are equal to the estimates of the deterministic method (i.e., the least squares estimation). With this error distribution, the likelihood function of the real components is given by

$$f(\mathrm{Re}[\rho^{obs}(\omega_k)] \mid \rho_0, \mathbf{m}, \mathbf{b}, \mathbf{c}, u_{re}) = \sqrt{\frac{u_{re}}{2\pi}} \exp\left(-\frac{u_{re}}{2} \left(\frac{\mathrm{Re}[\rho^{obs}(\omega_k)] - \mathrm{Re}[\rho(\omega_k)]}{\mathrm{Re}[\rho^{obs}(\omega_k)]} \right)^2 \right). \tag{7}$$

Similarly, we can define the likelihood function of the imaginary components of complex resistivity as

$$f(\mathrm{Im}[\rho^{obs}(\omega_k)] \mid \rho_0, \mathbf{m}, \mathbf{b}, \mathbf{c}, u_{im}) = \sqrt{\frac{u_{im}}{2\pi}} \exp\left(-\frac{u_{im}}{2} \left(\frac{\mathrm{Im}[\rho^{obs}(\omega_k)] - \mathrm{Im}[\rho(\omega_k)]}{\mathrm{Im}[\rho^{obs}(\omega_k)]} \right)^2 \right). \tag{8}$$

Prior models

The prior distribution of Cole-Cole parameters is determined from our prior knowledge or other information about the parameters, which may be subjective and site-specific. Because we assume that each parameter is independent of others, we can write the joint prior distribution given in equation (5) as the product of prior distributions of each individual parameter

$$f(\rho_0, \mathbf{m}, \mathbf{b}, \mathbf{c}, u_{re}, u_{im}) = f(\rho_0)\, f(\mathbf{m})\, f(\mathbf{b})\, f(\mathbf{c})\, f(u_{re})\, f(u_{im})\,. \tag{9}$$

To minimize subjectivity, we assume in this study that the parameters ρ_0, $\mathbf{m}$, $\mathbf{b}$, and $\mathbf{c}$ have uniform distributions over given ranges. For example, for the synthetic case studies presented in the section of synthetic studies, the prior ranges of the parameters ρ_0, $\mathbf{m}$, $\mathbf{b}$, and $\mathbf{c}$ are given as $(1,\ 1000)$ (in Ωm), $(-5,\ 0)$, $(-5,\ 5)$ ($\log\tau$, τ in s), and $(0,\ 1)$, respectively. We similarly use proper non-informative prior distributions for inverse variances u_{re} and u_{im} as done in the software of the Bayesian inference using Gibbs sampling (BUGS) (Spiegelhalter et al., 1994), which are the gamma distribution with both shape and inverse scale parameters of 1e-3. The above prior models are quite non-informative. As a result, the estimates of Cole-Cole parameters obtained from the stochastic method primarily depend on the data and thus are comparable to those obtained from the Gauss-Newton based deterministic method.

SAMPLING METHODS

We obtain the estimates of unknown parameters by drawing many samples from the joint posterior pdf defined in equation (5) using MCMC methods. MCMC methods provide a powerful approach for sampling multivariate variables from a complex joint probability distribution. They are superior over conventional Monte Carlo methods because the conventional methods draw independent samples and are prohibitive for drawing samples from high-dimensional joint distribution functions. As opposed to deterministic methods, which seek single optimal solutions of unknown parameters, MCMC sampling-based stochastic methods draw many samples from the joint posterior pdf. The obtained samples can then be used to infer statistics of each parameter, such as its mean, variance, and predictive intervals. As is described in the following subsections, we use different methods to draw samples from the joint posterior distribution for the Cole-Cole parameters, for the zero frequency resistivity, and for the inverse variance of data.

Conditional probability distributions of the Cole-Cole model parameters

We first derive the conditional pdfs of the Cole-Cole parameters $\mathbf{m}$, $\mathbf{b}$, and $\mathbf{c}$. Because the conditional distribution of each of those parameters is similar, in the following we only describe the method for obtaining the conditional distribution of the chargeability vector $\mathbf{m}$, given all other unknown parameters and SIP data. As MCMC sampling methods only concern the quantities that are functions of vector $\mathbf{m}$, we can obtain the conditional $f(\mathbf{m}\,|\,\cdot)$ by keeping those terms that are related to the vector $\mathbf{m}$. The result is given by

$$\begin{aligned} f(\mathbf{m}\,|\,\cdot) \propto \mathrm{Ind}(\mathbf{m} \in D_{\mathbf{m}}) \prod_{k=1}^{n} f(\mathrm{Re}[\rho^{obs}(\omega_k)]\,|\,\rho_0, \mathbf{m}, \mathbf{b}, \mathbf{c}, u_{re}) \\ \prod_{i=1}^{n} f(\mathrm{Im}[\rho^{obs}(\omega_k)]\,|\,\rho_0, \mathbf{m}, \mathbf{b}, \mathbf{c}, u_{im}). \end{aligned} \tag{10}$$

The first term on the right side of equation (10) is an indicator variable that accounts for the constraint from the prior distribution of vector $\mathbf{m}$, where $D_{\mathbf{m}}$ is the given prior range of chargeability. Similarly, we can obtain conditional pdfs of the Cole-Cole parameters $\mathbf{b}$ and $\mathbf{c}$.

Conditional probability distribution of the zero frequency resistivity

We can obtain the analytical form of the conditional pdf of the zero frequency resistivity because the real and imaginary components of SIP data are linear functions of it. We simplify equations (3) and (4) as $\mathrm{Re}[\rho(\omega_k)] = \rho_0 A(\omega_k)$ and $\mathrm{Im}[\rho(\omega_k)] = \rho_0 B(\omega_k)$ by letting $A(\omega_k) = 1 - \sum_{l=1}^{L} m_l \left(1 - \frac{R_l}{R_l^2 + I_l^2}\right)$ and $B(\omega_k) = -\sum_{l=1}^{L} m_l \frac{I_l}{R_l^2 + I_l^2}$. Consequently, the conditional pdf has a truncated normal distribution (see Appendix A) as given below

$$f(\rho_0\,|\,\cdot) \propto Ind(\rho_0 \in D_\rho)\; N(\mu_\rho^*, u_\rho^*), \tag{11}$$

where D_ρ is the given prior range of the zero frequency resistivity, and $u_\rho^* = u_{re} \sum_{k=1}^{n} \left(\frac{A(\omega_k)}{\mathrm{Re}[\rho^{obs}(\omega_k)]} \right)^2 + u_{im} \sum_{k=1}^{n} \left(\frac{B(\omega_k)}{\mathrm{Im}[\rho^{obs}(\omega_k)]} \right)^2$ and

$$\mu_\rho^* = \left(u_{re} \sum_{k=1}^{n} \frac{A(\omega_k)}{\mathrm{Re}[\rho^{obs}(\omega_k)]} + u_{im} \sum_{k=1}^{n} \frac{B(\omega_k)}{\mathrm{Im}[\rho^{obs}(\omega_k)]} \right) \frac{1}{u_\rho^*}.$$

Conditional probability distributions of the inverse variance of measurement errors

As the prior distributions of the inverse variances of measurement errors are conjugate priors for the likelihood models defined in equations (7) and (8), we can also obtain the analytical forms of their conditional distributions, which are gamma distributions (see Appendix B) as follows

$$\begin{aligned} f(u_{re}\,|\,\cdot) &\propto f(u_{re})\prod_{k=1}^{n} f(\mathrm{Re}[\rho^{obs}(\omega_k)]\,|\,\rho_0,\mathbf{m},\mathbf{b},\mathbf{c},u_{re}) \\ &\propto \Gamma(\alpha+0.5n,\ \lambda+0.5S_{re}), \end{aligned} \tag{12}$$

$$\begin{aligned} f(u_{im}\,|\,\cdot) &\propto f(u_{im})\prod_{k=1}^{n} f(\mathrm{Im}[\rho^{obs}(\omega_k)]\,|\,\rho_0,\mathbf{m},\mathbf{b},\mathbf{c},u_{im}) \\ &\propto \Gamma(\alpha+0.5n,\ \lambda+0.5S_{im}), \end{aligned} \tag{13}$$

where $\alpha=\lambda=1e-3$, $S_{re}=\sum_{k=1}^{n}\left(\dfrac{\mathrm{Re}[\rho^{obs}(\omega_k)]-\mathrm{Re}[\rho(\omega_k)]}{\mathrm{Re}[\rho^{obs}(\omega_k)]}\right)^2$,

and $S_{im}=\sum_{k=1}^{n}\left(\dfrac{\mathrm{Im}[\rho^{obs}(\omega_k)]-\mathrm{Im}[\rho(\omega_k)]}{\mathrm{Im}[\rho^{obs}(\omega_k)]}\right)^2$.

Sampling algorithm and monitoring convergence

We use the Gibbs sampler (Geman and Geman, 1984) to draw samples from the joint posterior distribution defined in equation (5). The main steps are list below

1. Assign initial values to ρ_0, $\mathbf{m}$, $\mathbf{b}$, $\mathbf{c}$, u_{re}, and u_{im}, and refer to them as $\rho_0^{(0)}$, $\mathbf{m}^{(0)}$, $\mathbf{b}^{(0)}$, $\mathbf{c}^{(0)}$, $u_{re}^{(0)}$, and $u_{im}^{(0)}$, respectively. Let $t=1$.
2. Draw a sample from $f(\rho_0\,|\,\cdot)$ given $\mathbf{m}^{(t-1)}$, $\mathbf{b}^{(t-1)}$, $\mathbf{c}^{(t-1)}$, $u_{re}^{(t-1)}$, and $u_{im}^{(t-1)}$, and refer to it as $\rho_0^{(t)}$.

3. Draw a sample from $f(\mathbf{m}\,|\,\cdot)$ given $\rho_0^{(t)}$, $\mathbf{b}^{(t-1)}$, $\mathbf{c}^{(t-1)}$, $u_{re}^{(t-1)}$, and $u_{im}^{(t-1)}$, and refer to it as $\mathbf{m}^{(t)}$.
4. Draw a sample from $f(\mathbf{b}\,|\,\cdot)$ given $\rho_0^{(t)}$, $\mathbf{m}^{(t)}$, $\mathbf{c}^{(t-1)}$, $u_{re}^{(t-1)}$, and $u_{im}^{(t-1)}$, and refer to it as $\mathbf{b}^{(t)}$.
5. Draw a sample from $f(\mathbf{c}\,|\,\cdot)$ given $\rho_0^{(t)}$, $\mathbf{m}^{(t)}$, $\mathbf{b}^{(t)}$, $u_{re}^{(t-1)}$, and $u_{im}^{(t-1)}$, and refer to it as $\mathbf{c}^{(t)}$.
6. Draw a sample from $f(u_{re}\,|\,\cdot)$ given $\rho_0^{(t)}$, $\mathbf{m}^{(t)}$, $\mathbf{b}^{(t)}$, $\mathbf{c}^{(t)}$, and $u_{im}^{(t-1)}$, and refer to it as $u_{re}^{(t)}$.
7. Draw a sample from $f(u_{im}\,|\,\cdot)$ given $\rho_0^{(t)}$, $\mathbf{m}^{(t)}$, $\mathbf{b}^{(t)}$, $\mathbf{c}^{(t)}$, and $u_{re}^{(t)}$, and refer to it as $u_{im}^{(t)}$.
8. Let $t = t+1$. If $t > T$, where T is the maximum number of iterations allowed, stop; otherwise, go to step 2.

We can obtain many samples of the unknown Cole-Cole parameters and inverse variances of measurement errors, i.e. $\left\{\rho_0{}^{(t)},\ \mathbf{m}^{(t)},\ \mathbf{b}^{(t)},\ \mathbf{c}^{(t)},\ u_{re}^{(t)},\ u_{im}^{(t)},\ t=1,2,\cdots,T\right\}$, by following the aforementioned algorithm. Theoretically, after a sufficiently long run (e.g., t_0 iterations, referred to as burn-in by Gilks et al., 1996), the drawn samples are approximately the samples drawn from the true joint pdf given in equation (5). Many methods can be used to find the burn-in number and to monitor the convergence of the obtained Markov chains, such as the methods developed by Gelman and Rubin (1992), Geweke (1992), and Raftery and Lewis (1992); we employ the Gelman and Rubin (1992) method in this study.

We run three different chains by starting from different sets of initial values for the total number of T iterations. As the samples drawn early in the process may depend on the starting values, we throw away the first $0.5T$ number of samples for each chain and consider them as the burn-in. We calculate a criterion, referred to as the scale reduction score in Gelman and Rubin (1992), based on the three Markov chains. With that approach, if the scale reduction score is less than 1.2, the Markov chain is considered to be converged; otherwise, more runs are needed.

SYNTHETIC STUDIES

We first demonstrate the use of the sampling-based Bayesian model for Cole-Cole parameter estimation using a synthetic SIP data set; we then compare the results obtained from the stochastic approach with those obtained from the deterministic method developed by Kemna (2000). We choose a synthetic case with a dual Cole-Cole model because this case is often encountered in practice, either to describe an SIP response with two relaxation domains or to describe a single-relaxation SIP response contaminated by capacitive and/or inductive coupling associated with the measurement layout (Pelton et al., 1978; Kemna et al., 1999).

True Cole-Cole model parameters and synthetic IP data

The synthetic Cole-Cole model parameters are listed in the second column of Table 2. These values are the same as those used by Cao et al. (2005), except for the zero frequency resistivity, whose value was not provided by the paper. The dual Cole-Cole model is mainly separated by the two chargeabilities, which have a ratio of 50. We generated synthetic SIP data using frequencies ranging from 1 mHz to 10 kHz as is typical of SIP measurements, and added 1% relative random noise to the real and imaginary components of the generated resistivity data.

This level of noise is reasonable based on noise distributions estimated from the laboratory SIP data presented in the section of laboratory studies.

Inversion procedure of the MCMC-based stochastic method

We start to invert the SIP data using common and wide (i.e., non-informative) prior ranges, specifically (1, 1000) (in Ωm) for the zero-frequency resistivity ρ_0, (1e-5, 1) for chargeabilities m_1 and m_2, (0, 1) for dependence factors c_1 and c_2, and (-5, 5) (in s) for base 10 logarithmic time constants $\log(\tau_1)$ and $\log(\tau_2)$ (see column 3 of Table 2). We run three Markov chains using the three sets of initial values given by the fourth, fifth, and sixth columns of Table 2. We run each chain by beginning with one of the three sets of initial values for 20,000 iterations and use the latter half to estimate the marginal posterior pdf of each Cole-Cole parameter. The CPU time for the sampling is on the order of minutes using a personal computer with 1.8 GHz speed.

Figure 1 shows the estimated marginal pdf of chargeability m_1, obtained stochastically using the synthetic SIP data with 1% relative noise. Two modes appear in the pdf: one is close to 0.0 and the other is around 0.5. This is because if we switch the values between the Cole-Cole parameters (m_1, τ_1, c_1) and (m_2, τ_2, c_2), the IP responses calculated from equations (3) and (4) do not change. To avoid the bimodality, we re-run the Markov chains by modifying the prior ranges of chargeability as follows, (0.25, 1) for m_1 and (1e-5, 0.25) for m_2. Using such a two-step procedure, we obtain the marginal posterior pdfs of all the Cole-Cole parameters with a unique mode.

Comparison between the stochastic and deterministic inversion methods

In this subsection, we explore how the choice of initial values impacts the deterministic and stochastic estimation results, and assess the uncertainty information provided by both inversion methods.

Dependence on the choice of initial values

The choice of initial values is not critical for the stochastic inversion method because it affects only the speed of convergence of Markov chains to the target probability distribution function being sampled, but not the inversion result. In fact, it is essential for the MCMC-based methods to run multiple chains with very different sets of initial values in order to avoid possible local convergence. Although the stochastic method provides extensive information about each unknown parameter, we use only the medians as the best estimates and compare them with the estimates obtained from the deterministic method. In the third column of Table 3, we show the estimated medians of unknown Cole-Cole parameters based on all the three Markov chains obtained using the three initial sets given in Table 2 because the estimated medians from each individual chain are almost identical. From the comparison between the estimated medians and their corresponding true values, which are given in the second column of the same table, we can see that even if we start from very different initial values, the MCMC based method can provide good estimates of unknown parameters.

The choice of initial values is critical for the deterministic inversion, especially when considering a multiple Cole-Cole model. We found that the method often can not converge given an arbitrary choice of initial values. For example, when we applied the initial values given in Table 2 for the stochastic inversion to the deterministic inversion method, none could converge to a solution that was close to the true values. A main problem caused by the dependence of the estimates on the initial values is that if differences between resultant data misfits for estimates obtained from different sets of initial values are subtle, it is difficult to decide which solution should be preferred without knowing the probability of the parameter sets.

Table 3 shows the estimates of Cole-Cole parameters obtained deterministically using different sets of initial values. The first one is listed in the last column of Table 2, obtained after several tries by observing the SIP data fits without knowing the true values, and the second one uses the true values of the synthetic model. Figure 2 shows the fits to the synthetic SIP data with 1% relative noise using the deterministic approach with these two different sets of initial values, together with the fit obtained from the stochastic method. If we did not know the true model parameters, given 1% relative noise in the data, we may be satisfied with the estimates obtained from the first set of initial values. However, comparison with the true Cole-Cole parameters shows that the results in column 4 of Table 3, having the root mean square of errors (RMS) of 0.57, is clearly worse than the results in column 3 of the same table, having the RMS of 0.084 and obtained from the stochastic inversion method. The estimates found from the second set of initial values (column 5 in Table 3) are better (RMS=0.065) and represent the global solution of the inverse problem because we started from the true Cole-Cole parameters; these estimates are comparable with those (column 3 in Table 3) obtained from the stochastic inversion method.

In practice, we rarely have enough a-priori information about SIP mechanisms to choose good initial values that are close enough to the true values to lead to a global optimal solution using the deterministic approach. However, we may desire a single parameter estimate rather than a pdf. We can achieve both goals by using a combination of the stochastic and deterministic approaches, whereby we initialize the deterministic method using the medians of the stochastically obtained marginal posterior pdfs. The sixth column of Table 3 illustrates this approach, and indicates that the obtained estimates are indeed very close (RMS=0.072) to the true Cole-Cole parameters, which are just slightly worse than the results obtained by starting from the true values (RMS=0.065).

Estimated uncertainty information

The stochastic method can provide the entire estimated posterior pdfs and hence extensive information of the unknown parameters. To compare the stochastic estimation results with those obtained using the deterministic method, we use only the 95% highest probability domain (HPD) of unknown parameters as a measure of uncertainty, which is equivalent to the 95% confidence intervals (CIs) in the deterministic inversion method. Table 4 shows the 95% HPD of Cole-Cole parameters obtained from the stochastic method and the 95% CIs of estimated parameters from the deterministic inversion method. Note that the upper bound of the possible c_2 range was also set to 1 in the deterministic approach. This table suggests that the stochastic method provides very high precision for all the unknown variables; the true values are all within the 95% HPD.

The quality of uncertainty information obtained from the deterministic method varies, depending on the obtained optimal solutions. For the initial values given in the last column of Table 2, the resultant estimates do not represent a global solution, as shown in Table 3 and Figure 3. Their 95% CIs are very wide; some even do not include the true values. For example, the deterministically-obtained time constant τ_2 and dependence factor c_2 shown in Figure 3 vary significantly from the true value. However, when the initial values are well chosen (i.e., close to the true values), the deterministic method provides good uncertainty information. For example, when the initial values for the deterministic approach are the true values or the medians of the stochastic results, the resulting 95% CIs are comparable to those obtained from the stochastic method (except for the zero frequency resistivity ρ_0).

The uncertainty information obtained from the stochastic method is different from that obtained from the deterministic method by definition. The uncertainty information of the stochastic method depends on the measurement errors in the data and the prior distributions, whereas the uncertainty information of the deterministic method is a function of the measurement errors in the data and is related to the obtained solution. If the estimated values are close to the true values, the 95% CIs are tight; otherwise, they are inaccurate, as shown in Table 4. For the stochastic method, as long as the Markov chains converge, we can get good estimates of uncertainty information about the unknown parameters.

LABORATORY STUDIES

Spectral IP laboratory measurements

We use two laboratory SIP data sets measured on unconsolidated sediment samples to compare the performance of the deterministic and stochastic methods for Cole-Cole parameter estimation. The first data set (Figure 4) was measured on a silica sand sample that has grain size of 125-250 μm and was saturated with a 3×10^{-4} molar KCl solution (Kemna et al., 2005). The data show a Cole-Cole type behavior in the low to moderate frequency range (i.e., below 100 Hz) at relatively low polarizability as is typical of silica sands. Note that the decrease of the real part of resistivity towards lowest frequencies (i.e., below 30 mHz) is due to ions being detached from the matrix and going into solution during data acquisition time, which is of the order of two hours for this frequency range. Towards higher frequencies (i.e., above 100 Hz), the data are increasingly dominated by capacitive coupling effects associated with the measurement setup, as typical in impedance spectroscopy. These coupling effects may be described by the low-frequency branch of a higher-frequency Cole-Cole dispersion term (Kemna et al., 2000).

The second data set (Figure 5) was collected from a sample that was extracted from a sand/gravel aquifer at the Krauthausen test site in Germany (Kemna et al., 2002; Hördt et al., 2007), using the same device and experimental setup as for the first set of laboratory measurements. The sample was saturated with water having an electrical conductivity of approximately 0.05 S/m. The fluvial aquifer at the site partly exhibits a strongly non-uniform grain size distribution. This is reflected in the selected data set, where two Cole-Cole type dispersion regions can be identified with phase peaks at approximately 0.1 Hz and 100 Hz, again superimposed by a continuous phase shift increasing towards higher frequencies (i.e., above 1 kHz) due to capacitive coupling associated with the measurement layout.

Inversion of the SIP data from the silica sand sample

We first inverted the SIP data obtained from the silica sand sample using the deterministic method for a dual Cole-Cole model. After trying several sets of initial values, we chose the values given in the second column of Table 5. The corresponding estimates of the Cole-Cole parameters and their associated 95% CIs are listed in the third and fourth columns of the same table, respectively. The estimated Cole-Cole parameters seem to fit the SIP data well as shown by the red curves in Figure 4. For ease of comparison, we calculate the relative half width (RHW) of 95% confidence intervals by normalizing each actual half width by the absolute value of its corresponding optimal estimate. We can see that the obtained confidence intervals of the estimates overall are tight (RHW<6%), except for those of m_2 (RHW=101%), $\log(\tau_1)$ (RHW=10%), and $\log(\tau_2)$ (RHW=25%). Note that the lower bound of the possible m_2 range was set to 0.

We also inverted the same SIP data set for a dual model using our stochastic method. We used common prior ranges for the two sets of Cole-Cole model parameters, i.e., (1, 1000) (in

Ωm) for zero-frequency resistivity, (-5, 0) ($\log(m)$) for chargeability, (-10, 10) ($\log(\tau)$, τ in s) for time constant, and (0, 1) for dependence factor. Following the two-step procedure described in the section of synthetic studies, we obtained the estimated marginal posterior pdfs of the Cole-Cole parameters. For comparison with the deterministic result, we list the medians and their corresponding 95% HPDs in Table 5. Except for chargeability m_2 and time constant $\log(\tau_2)$, which are poorly constrained by the data, the medians of the estimated posterior pdfs of the Cole-Cole parameters are very close to those obtained from the deterministic method. However, the stochastic method provides much tighter uncertainty bounds for those estimates; all the relative half widths of 95% HPDs are less than 3%, except for those of m_2 (RHW=52%), $\log(\tau_1)$ (RHW=4%), and $\log(\tau_2)$ (RHW=5%).

Figure 6 compares the estimated pdfs of the Cole-Cole parameters obtained from the stochastic method with the optimal estimates obtained from the deterministic method. Except for the time constant $\log(\tau_2)$ and the dependence factor c_2, the estimates obtained from the deterministic method are all within the HPDs of the posterior pdfs. To demonstrate the effect of initial values, we inverted the same data set using the deterministic method starting from the medians of our posterior pdfs. The corresponding new estimates are also shown in Figure 6. Note that all the estimated Cole-Cole parameters now are very close to the medians of the estimated marginal posterior pdfs. The new estimates represent a better solution in terms of the Chi-square misfit, which is 0.44 for the original initial values and 0.37 for the new initial values.

Table 6 compares the correlation coefficients of Cole-Cole parameters obtained from the deterministic (above slashes) and the stochastic (below slashes) methods. Both methods give us very small values of cross-correlation between the zero-frequency resistivity and other parameters. In addition, we can see that the stochastic method provides very similar but slightly smaller values of cross-correlation among the parameters (m_1, $\log(\tau_1)$, c_1), which are reasonably constrained by the data, than does the deterministic method. However, the differences in cross-correlations between parameters involving m_2, $\log(\tau_2)$, or c_2 are quite large, which may be contributed to the poor resolvability of particularly m_2 and $\log(\tau_2)$.

Inversion of the SIP data from the Krauthausen sand/gravel sample

We also inverted the SIP data obtained from the sand and gravel sample from the Krauthausen site using the deterministic and stochastic methods. For the deterministic method, we fitted the data with a triple Cole-Cole model after several tries with different initial values. Table 7 shows the initial values, the obtained estimates, and the 95% CIs of the estimates. As shown in Figure 5, the estimated Cole-Cole parameters seem to fit the complex resistivity data very well. As in the example before, chargeability and time constant of the highest-frequency Cole-Cole terms (i.e., m_3 and $\log(\tau_3)$) are effectively not resolved (i.e., exhibit huge 95% CIs, for m_3, the CI is actually given by the pre-set lower and upper bounds of the allowed range), as expected from the spectral behavior of the data (Figure 5).

For the stochastic method, we also inverted for the triple Cole-Cole model parameters using the common prior ranges. The medians and the 95% HPDs of the Cole-Cole parameters are given in the fifth and sixth columns of Table 7. Similarly, the medians of the estimated pdfs are very close to the optimal solution obtained from the deterministic inversion method, except for m_3 and $\log(\tau_3)$. As shown in Figure 7, the estimates of the Cole-Cole parameters from the deterministic approach are all very close to the modes of the estimated marginal pdfs. This means that the optimal estimates found by the deterministic method likely represent a global solution for the triple Cole-Cole model. Again, the uncertainty bounds estimated from the deterministic method are much wider than those obtained from the stochastic method as shown in Table 7. If we assume that the true model indeed is a triple model, the estimated relative errors of real and imaginary components of the SIP data are 0.5% and 1.9%, respectively, both of which are quite small.

CONCLUSIONS

We have developed an MCMC based Bayesian model to invert for Cole-Cole parameters from SIP data and have compared its performance with the commonly used deterministic (Gauss-Newton) method through inversion of synthetic and laboratory data. The Bayesian method estimates the marginal posterior pdfs of Cole-Cole parameters using samples obtained from the joint posterior pdf defined by the likelihood functions of SIP data and prior distributions of unknown parameters, whereas the deterministic method seeks the optimal solution by minimizing the squared misfit of the model response with the SIP data. We use non-informative priors in the stochastic method, the estimates of Cole-Cole parameters obtained from the stochastic method primarily depend on the data and thus can be compared to those obtained from the deterministic method. Through detailed comparison between the stochastic and deterministic inversion methods for inverting synthetic and laboratory SIP data, we found that the sampling based stochastic method has two key advantages over the deterministic method.

The first advantage is that the stochastic method provides a global approach for inverting SIP data for Cole-Cole parameters; the obtained estimates are independent of initial values. The deterministic method is a localized approach for inverting the SIP data by finding an optimal solution that fits the SIP data through iteratively updating the model from a starting model of initial values, which typically need to be very close to the true model parameters. Because of the nonlinearity of the forward Cole-Cole modeling and the general non-uniqueness and ill-posed nature of the inverse problem, many local optimal solutions may exist. Consequently, as demonstrated in the synthetic and laboratory data analyses, different initial values can yield different solutions with similar misfit criteria. The MCMC sampling based stochastic method virtually can start from a wide range of initial values; the obtained Markov chains converge to the target probability distribution function. Indeed, it is good to run Markov chains from several very different sets of initial values in order to detect possible local convergence.

The second advantage is that the stochastic method provides a better way to quantify uncertainty in the inverse problem. The deterministic method estimates the uncertainty of unknown parameters from the diagonal terms of the covariance matrix that is determined by both the regularization and the Jacobian matrices evaluated at a presumed optimal solution. The precision of such estimation depends on whether the found minimum is a local or a global minimum and the local characteristics (e.g., nonlinearity and non-uniqueness) of the solution. If the minimum indeed is a local minimum, the estimated uncertainties of the parameters are wrong. In contrast, the stochastic method estimates the uncertainty of unknown parameters using an Monte Carlo approach. We use MCMC sampling methods to draw many samples of unknown parameters from the joint posterior pdf. As long as those Markov chains converge to the target pdf, the obtained uncertainty information about the unknown parameter is global information, independent of the choice of initial values and the local characteristics of specific solutions.

The MCMC based inversion methods compared to the Gauss-Newton based inversion methods potentially have two downsides. The first one is that the computation time for the MCMC method is couple of orders larger than that of deterministic methods. But for IP data inversion, it is not an issue because the running time for deterministic methods is in the order of seconds and that of stochastic methods is in the order of minutes on a PC or laptop, which is acceptable. The second possible limitation of stochastic methods is that they provide marginal probability distribution but not optimal solutions like the deterministic methods. The users may pick the mean, median, or the mode of the marginal probability distribution as the optimal estimate of unknown parameters. The two methods can complement each other; for example, we can use stochastic methods to find the distribution and use the medians or modes as initial values for the Gauss-Newton methods to pick one set of optimal solution.

APPENDIX A -- Derivation of conditional distribution of the zero frequency resistivity

The derivation of equation (11) is given below

$$
\begin{aligned}
f(\rho_0 \mid \cdot) &\propto Ind(\rho_0 \in D_\rho) \\
&\qquad \exp\left\{ \text{-}0.5 \sum_{k=1}^{n} \left[u_{re} \left(1 - \frac{A(\omega_k)}{\mathrm{Re}[\rho^{obs}(\omega_k)]} \rho_0 \right)^2 + u_{im} \left(1 - \frac{B(\omega_k)}{\mathrm{Im}[\rho^{obs}(\omega_k)]} \rho_0 \right)^2 \right] \right\} \\
&\propto \mathrm{Ind}(\rho_0 \in D_\rho) \\
&\qquad \exp\left\{ \text{-}0.5 \left[u_{re} \sum_{k=1}^{n} \left(\frac{A(\omega_k)}{\mathrm{Re}[\rho^{obs}(\omega_k)]} \right)^2 + u_{im} \sum_{k=1}^{n} \left(\frac{B(\omega_k)}{\mathrm{Im}[\rho^{obs}(\omega_k)]} \right)^2 \right] \rho_0^2 \right\} \\
&\qquad \exp\left\{ \left[u_{re} \sum_{k=1}^{n} \left(\frac{A(\omega_k)}{\mathrm{Re}[\rho^{obs}(\omega_k)]} \right) + u_{im} \sum_{k=1}^{n} \left(\frac{B(\omega_k)}{\mathrm{Im}[\rho^{obs}(\omega_k)]} \right) \right] \rho_0 \right\} \\
&\propto Ind(\rho_0 \in D_\rho) \exp\left\{ -\frac{u_\rho^*}{2} \left(\rho_0 - \mu_\rho^* \right)^2 \right\} \\
&\propto Ind(\rho_0 \in D_\rho)\ N(\mu_\rho^*, u_\rho^*)
\end{aligned}
\tag{A-1}
$$

APPENDIX B -- Derivation of conditional distributions of the inverse variances

The gamma distribution is a conjugate prior for the multivariate normal likelihood function defined in equations (7) and (8), hence the posterior distributions of the inverse variances of the measurement errors are also gamma distributions as given below

$$
\begin{aligned}
f(u_{re} \mid \cdot) &\propto f(u_{re}) \prod_{k=1}^{n} f(\mathrm{Re}[\rho^{obs}(\omega_k)] \mid \rho_0, \mathbf{m}, \mathbf{b}, \mathbf{c}, u_{re}) \\
&\propto \left\{ u_{re}^{\alpha-1} \exp(-\lambda u_{re}) \right\} \left\{ u_{re}^{0.5n} \exp\left(-0.5 u_{re} \sum_{k=1}^{n} \left(\mathrm{Re}[\rho^{obs}(\omega_k)] - \mathrm{Re}[\rho(\omega_k)] \right)^2 \right) \right\} \\
&\propto u_{re}^{(\alpha+0.5n)-1} \exp\left\{ -(\lambda + 0.5 S_{re}) u_{re} \right\} \\
&\propto \Gamma(\alpha + 0.5n,\ \lambda + 0.5 S_{re}).
\end{aligned}
\tag{B-1}
$$

Similarly,

$$
\begin{aligned}
f(u_{im} \mid \cdot) &\propto f(u_{im}) \prod_{k=1}^{n} f(\mathrm{Im}[\rho^{obs}(\omega_k)] \mid \rho_0, \mathbf{m}, \mathbf{b}, \mathbf{c}, u_{im}) \\
&\propto \left\{ u_{im}^{\alpha-1} \exp(-\lambda u_{im}) \right\} \left\{ u_{im}^{0.5n} \exp\left(-0.5 u_{im} \sum_{k=1}^{n} \left(\mathrm{Im}[\rho^{obs}(\omega_k)] - \mathrm{Im}[\rho(\omega_k)] \right)^2 \right) \right\} \qquad \text{(B–2)} \\
&\propto u_{im}^{(\alpha+0.5n)-1} \exp\left\{ -(\lambda + 0.5 S_{im}) u_{im} \right\} \\
&\propto \Gamma(\alpha + 0.5n,\ \lambda + 0.5 S_{im}).
\end{aligned}
$$

ACKNOWLEDGMENTS

This study was funded by the U.S. Department of Energy, Environmental Remediation Science Program (ERSP), under Contract No. DE-AC02-05CH11231 to LBNL.. We thank Martin Münch (formerly ICG-4, Forschungszentrum Jülich, Germany) and Odilia Esser (ICG-4, Forschungszentrum Jülich, Germany) who helped with the laboratory SIP measurements included in this study. We also thank the associate editor Dr. John Bradford, Dr. Louise Pellerin, and two anonymous reviewers for their insightful comments and suggestions.

REFERENCES

Binley, A., L. D. Slater, M. Fukes, and G. Cassiani, 2005, Relationship between spectral induced polarization and hydraulic properties of saturated and unsaturated sandstone: Water Resources Research, **41**, W12417.

Boadu, F. K., and B. Seabrook, 2000, Estimating hydraulic conductivity and porosity of soils from spectral electrical response measurements: Journal of Environmental and Engineering Geophysics, **5**, 1-9.

Bosch, M., 1999, Lithologic tomography: From plural geophysical data to lithology estimation: Journal of Geophysical Research, **104**, 749-766.

Buland, A., and H. Omre, 2003, Bayesian linearized AVO inversion: Geophysics, **68**, 185-198.

Cao, Z., Y. Chang, and Y. Luo, 2005, Inversion study of spectral induced polarization based on improved genetic algorithm: Progress in Electromagnetics Research Symposium (PIERS) Online, **1**, 266-270; http://piers.mit.edu/piersonline/piers.php.

Chen J., S. Hubbard, Y. Rubin, C. Murray, E. Roden, and E. Majer, 2004, Geochemical characterization using geophysical data and Markov chain Monte Carlo methods: A case study at the South Oyster Bacterial Transport Site in Virginia: Water Resources Research, **40**, W12412.

Chen, J., S. Hubbard, J. Peterson, K. Williams, M. Fienen, P. Jardine, and D. Watson, 2006, Development of a joint hydrogeophysical inversion approach and application to a contaminated fractured aquifer: Water Resources Research, **42**, W06425.

Cole, K. S., and R. H. Cole, 1941, Dispersion and absorption in dielectrics I: Alternating current field: Journal of Chemical Physics, **1**, 341-351.

Gelman, A., and D. B. Rubin, 1992, Inference from iterative simulation using multiple sequences: Statistical Science, **7**, 457-472.

Geman, S., and D. Geman, 1984, Stochastic relaxation, Gibbs distribution, and Bayesian restoration of images: IEEE Transactions on Pattern Analysis and Machine Intelligence, **6**, 721-741.

Geweke, J., 1992, Evaluating the accuracy of sampling-based approaches to the calculation of posterior moments, *in* J. M. Bernardo, J. O. Berger, A. P. David, and A. F. M. Smith, eds., Bayesian statistics 4: Oxford University Press, 169-193.

Ghorbani, A., C. Camerlynck, N. Florsch, P. Cosenza, and A. Revil, 2007, Bayesian inference of the Cole-Cole parameters from time and frequency domain induced polarization: Geophysical Prospecting, **55**, 589-605.

Gilks, W. R., S. Richardson, and D. J. Spiegelhalter, 1996, Markov chain Monte Carlo in practice: Chapman and Hall.

Gunning, J., and M. E. Glinsky, 2004, Delivery: an open-source model-based Bayesian seismic inversion program: Computers and Geosciences, **30**, 619-636.

Hördt, A., R. Blaschek, A. Kemna, and N. Zisser, 2007, Hydraulic conductivity estimation from induced polarization data at the field scale – The Krauthausen case history: Journal of Applied Geophysics, **62**, 33-46.

Jaggar, S. R., and P. A. Fell, 1988, Forward and inverse Cole-Cole modeling in the analysis of frequency domain electrical impedance data: Exploration Geophysics, **19**, 463-470.

Kemna, A., E. Räkers, and L. Dresen, 1999, Field applications of complex resistivity tomography: 69th Annual International Meeting, SEG, Expanded Abstracts, 331-334.

Kemna, A., 2000, Tomographic inversion of complex resistivity: theory and application: Ph.D. thesis, Bochum Ruhr-University.

Kemna, A., A. Binley, A. Ramirez, and W. Daily, 2000, Complex resistivity tomography for environmental applications: Chemical Engineering Journal, **77**, 11-18.

Kemna, A., J. Vanderborght, B. Kulessa, and H. Vereecken, 2002, Imaging and characterization of subsurface solute transport using electrical resistivity tomography (ERT) and equivalent transport models: Journal of Hydrology, **267**, 125-146.

Kemna, A., H. M. Münch, K. Titov, E. Zimmermann, and H. Vereecken, 2005, Relation of SIP relaxation time of sands to salinity, grain size and hydraulic conductivity: 11th European Meeting of Environmental and Engineering Geophysics, EAGE, Extended Abstracts, P054.

Leroy, P., A. Revil, A. Kemna, P. Cosenza, and A. Ghorbani, 2008, Complex conductivity of water-saturated packs of glass beads: Journal of Colloid and Interface Science, **321**, 103-117.

Lesmes, D. P., and S. P. Friedman, 2005, Relationships between the electrical and hydrogeological properties of rocks and soils, *in* Y. Rubin, and S. Hubbard, eds., Hydrogeophysics: Springer, 87-128.

Luo, Y., and G. Zhang, 1998, Theory and application of spectral induced polarization: SEG Geophysical Monograph, **8**.

Mansoor, N., and L. Slater, 2007, On the relationship between iron concentration and induced polarization in marsh soils: Geophysics, **72**, no. 1, A1-A5.

Pelton, W. H., S. H. Ward, P. G. Hallof, W. R. Sill, and P. H. Nelson, 1978, Mineral discrimination and removal of inductive coupling with multi-frequency IP: Geophysics, **43**, 588-609.

Pelton, W. H., W. R. Sill, and B. D. Smith, 1984, Interpretation of complex resistivity and dielectric data, Part II: Geophysical Transactions, **30**, 11-45.

Raftery, A. E., and S. Lewis, 1992, How many iterations in the Gibbs sampler, *in* J. M. Bernardo, J. O. Berger, A. P. David, and A. F. M. Smith, eds., Bayesian statistics 4: Oxford University Press, 763-773.

Roy, I. G., 1999, An efficient nonlinear least squares 1D inversion scheme for resistivity and IP sounding data: Geophysical Prospecting, **47**, 527-550.

Scott, J. B., and R. D. Barker, 2003, Determining pore-throat size in Permo-Triassic sandstones from low-frequency electrical spectroscopy: Geophysical Research Letters, **30**, 1450, doi:10.1029/2003GL016951.

Slater, L. D., and D. Lesmes, 2002, IP interpretation in environmental investigations: Geophysics, **67**, 77-88.

Slater, L. D., J. Choi, and Y. Wu, 2005, Electrical properties of iron-sand columns: Implications for induced polarization investigation and performance monitoring of iron-wall barriers: Geophysics, **70**, no. 4, G87-G94.

Slater, L. D., D. Ntarlagiannis, and D. Wishart, 2006, On the relationship between induced polarization and surface area in metal-sand and clay-sand mixtures: Geophysics, **71**, no. 2, A1-A5.

Slater, L., 2007, Near surface electrical characterization of hydraulic conductivity: from petrophysical properties to aquifer geometries – A review: Surveys in Geophysics, **28**, 169-197.

Spiegelhalter, D. J., K. R. Abrams, N. G. Best, W. R. Gilks, and D. Lunn, 1994, Bayesian inference using Gibbs sampling (BUGS): MRC Biostatistics Unit, Cambridge, England; http://www.mrc-bsu.cam.ac.uk/bugs/.

Tarasov, A., and K. Titov, 2007, Relaxation time distribution from time domain induced polarization measurements: Geophysical Journal International, **170**, 31-43.

Titov, K., V. Komarov, V. Tarasov, and A. Levitski, 2002, Theoretical and experimental study of time domain-induced polarization in water-saturated sands: Journal of Applied Geophysics, **50**, 417-433.

Tong, M., L. Li, W. Wang, and Y. Jiang, 2006, Determining capillary-pressure curve, pore-size distribution, and permeability from induced polarization of shaley sand: Geophysics, **71**, no. 3, N33-N40.

Vanhala, H., 1997, Mapping oil-contaminated sand and till with the spectral induced polarization (SIP) method: Geophysical Prospecting, **45**, 303-326.

Xiang, J., N. B. Jones, D. Cheng, and F. S. Schlindwein, 2001, Direct inversion of the apparent complex-resistivity spectrum: Geophysics, **66**, 1399-1404.

FIGURE CAPTIONS

Figure 1: Estimated chargeability (m_1) for synthetic dual Cole-Cole model data using the common prior ranges.

Figure 2: Synthetic SIP data with 1% relative noise and obtained fits using the stochastic method (green curves) and the deterministic method for two sets of initial values (blue curves represent true values, and red curves represent Init0 values in Table 2) for a dual Cole-Cole model.

Figure 3: Comparison between estimated pdfs from the stochastic method (black curves) and estimated parameters from the deterministic method for three sets of initial values (blue lines represent true values, green lines represent medians of the stochastic results, and red lines represent Init0 values in Table 2) for the synthetic SIP data with 1% relative noise using a dual Cole-Cole model.

Figure 4: Silica-sand SIP data and fits obtained using the stochastic method (blue curves) and deterministic method (red curves) for a dual Cole-Cole model.

Figure 5: Krauthausen SIP data and fits obtained using the stochastic method (blue curves) and deterministic (red curves) method for a triple Cole-Cole model.

Figure 6: Comparison between estimated pdfs from the stochastic method (black curves) and estimated parameters from the deterministic method for two sets of initial parameters (blue lines represent medians of the stochastic results, red lines represent values found from test tries) for the silica-sand SIP data using a dual Cole-Cole model.

Figure 7: Comparison between estimated pdfs from the stochastic method (black curves) and the estimated parameters from the deterministic method (red lines) for Krauthausen SIP data using a triple Cole-Cole model.

Table 1. True Cole-Cole parameters of the synthetic dual model, the prior ranges and initial values of the stochastic method, and the initial values of the deterministic method for inverting the synthetic SIP data

Cole-Cole	True	Stochastic Inversion				Deterministic Inversion
Parameters	Values	Prior Ranges	Initial-1	Initial-2	Initial-3	Initial Values (Init0)
ρ_0 (Ωm)	25.0	(1,1000)	5	50	500	20
m_1	0.5	(1e-5,1)	0.1	0.4	0.6	0.1
$log(\tau_1)$ (τ_1 in s)	1.0	(-5,5)	-4	-1	1	1
c_1	0.4	(0,1)	0.1	0.4	0.6	0.5
m_2	0.01	(1e-5,1)	0.1	0.4	0.6	0.1
$log(\tau_2)$ (τ_2 in s)	0	(-5,5)	-4	-1	1	-1
c_2	0.98	(0,1)	0.1	0.4	0.6	0.5

Table 2. Comparison of the estimates from inversion of the SIP data with 1% relative noise using the stochastic and deterministic methods

Cole-Cole Parameters	True Values	Stochastic Inversion Medians	Deterministic Inversion		
			Estimates (Using Init0)	Estimates (Using True Values)	Estimates (Using Medians)
$\rho_0(\Omega m)$	25	25.01	24.92	25.01	25.02
m_1	0.5	0.496	0.410	0.490	0.490
$\log(\tau_1)$ (τ_1 in s)	1.0	1.009	0.878	1.009	1.012
c_1	0.4	0.398	0.416	0.398	0.397
m_2	0.01	0.015	0.1	0.016	0.017
$\log(\tau_2)$ (τ_2 in s)	0	0.147	1.218	0.137	0.145
c_2	0.98	0.836	0.311	0.896	0.881

Table 3. Comparison of uncertainty information obtained from inversion of the synthetic SIP data with 1% relative noise using the stochastic and deterministic methods

Cole-Cole Parameters	True Values	Stochastic Inversion 95% HPD	Deterministic Inversion 95% CI (Using Init0)	Deterministic Inversion 95% CI (Using True Values)	Deterministic Inversion 95% CI (Using Medians)
ρ_0 (Ωm)	25	(24.89,25.15)	(22.94,26.90)	(23.04,26.97)	(23.05,26.98)
m_1	0.5	(0.475,0.504)	(0,0.869)	(0.484,0.496)	(0.483,0.497)
$\log(\tau_1)$ (τ_1 in s)	1.0	(0.974,1.066)	(0.538,1.218)	(0.983,1.034)	(0.986,1.038)
c_1	0.4	(0.390,0.402)	(0.352,0.480)	(0.395,0.401)	(0.393,0.401)
m_2	0.01	(0.007,0.037)	(0,0.567)	(0.013,0.019	(0.014,0.020)
$\log(\tau_2)$ (τ_2 in s)	0.0	(-0.008,0.337)	(0.049,2.387)	(-0.092,0.366)	(-0.087,0.377)
c_2	0.98	(0.635,1.0)	(0.114,0.508)	(0.738,1.0)	(0.726,1.0)

Table 4. Comparison of inversion results using the deterministic and stochastic methods for the silica sand SIP data

Parameters	Deterministic method			Stochastic method	
	Initial Values	Estimates	95% CI	Medians	95%HPD
ρ_0 (Ωm)	770.77	773.40	(752.96,794.39)	773.33	(772.38,774.37)
m_1	1e-3	6.94e-3	(6.77e-3,7.11e-3)	6.90e-3	(6.7e-3,7e-3)
$\log(\tau_1)$ (τ_1 in s)	-1	-0.992	(-1.095,-0.889)	-0.972	(-1.005,-0.933)
c_1	0.5	0.418	(0.406,0.429)	0.423	(0.413,0.433)
m_2	1e-1	1.29e-1	(0,2.62e-1)	6.71e-1	(3.05e-1,1)
$\log(\tau_2)$ (τ_2 in s)	-6	-6.406	(-7.989,-4.823)	-7.462	(-7.734,-6.948)
c_2	1.0	0.765	(0.725,0.804)	0.736	(0.719,0.754)

Table 5. Comparison of correlation coefficients obtained from the deterministic and stochastic methods for the silica sand SIP data

Parameters	ρ_0	m_1	$\log(\tau_1)$	c_1	m_2	$\log(\tau_2)$	c_2
ρ_0	1						
m_1	0.01/-0.04	1					
$\log(\tau_1)$	0.00/0.01	-0.69/-0.62	1				
c_1	0.00/-0.02	-0.67/-0.63	0.64/0.60	1			
m_2	-0.01/-0.01	-0.51/-0.12	0.51/0.13	0.39/0.10	1		
$\log(\tau_2)$	0.01/0.01	0.52/0.19	-0.52/-0.20	-0.40/-0.16	-0.99/-0.97	1	
c_2	0.01/0.00	0.66/0.59	-0.67/-0.60	-0.53/-0.50	-0.89/-0.33	0.91/0.46	1

Table 6. Comparison of inversion results using the deterministic and stochastic methods for the Krauthausen data

Parameters	Deterministic method			Stochastic method	
	Initial Values	Estimates	95% CI	Medians	95% HPD
ρ_0 (Ωm)	98.49	98.38	(95.78,101.05)	98.37	(98.25,98.50)
m_1	5e-3	3.38e-3	(2.69e-3,4.07e-3)	3.4e-3	(3.2e-3,3.6e-3)
$\log(\tau_1)$ (τ_1 in s)	0	0.283	(-0.024,0.590)	0.285	(0.239,0.329)
c_1	0.5	0.58	(0.527,0.633)	0.580	(0.562,0.599)
m_2	2e-2	1.97e-2	(1.10e-2,2.83e-2)	1.97e-2	(1.82e-2,2.12e-2)
$\log(\tau_2)$ (τ_2 in s)	-3	-3.13	(-3.876,-2.384)	-3.134	(-3.201,-3.067)
c_2	0.5	0.492	(0.425,0.558)	0.491	(0.474,0.510)
m_3	2e-1	3.66e-1	(0,1)	5.318e-1	(1.753e-1,9.96e-1)
$\log(\tau_3)$ (τ_3 in s)	-7	-7.998	(-60.318,44.322)	-8.325	(-8.988,-7.263)
c_3	1.0	0.551	(0.425,0.558)	0.551	(0.504,0.604)

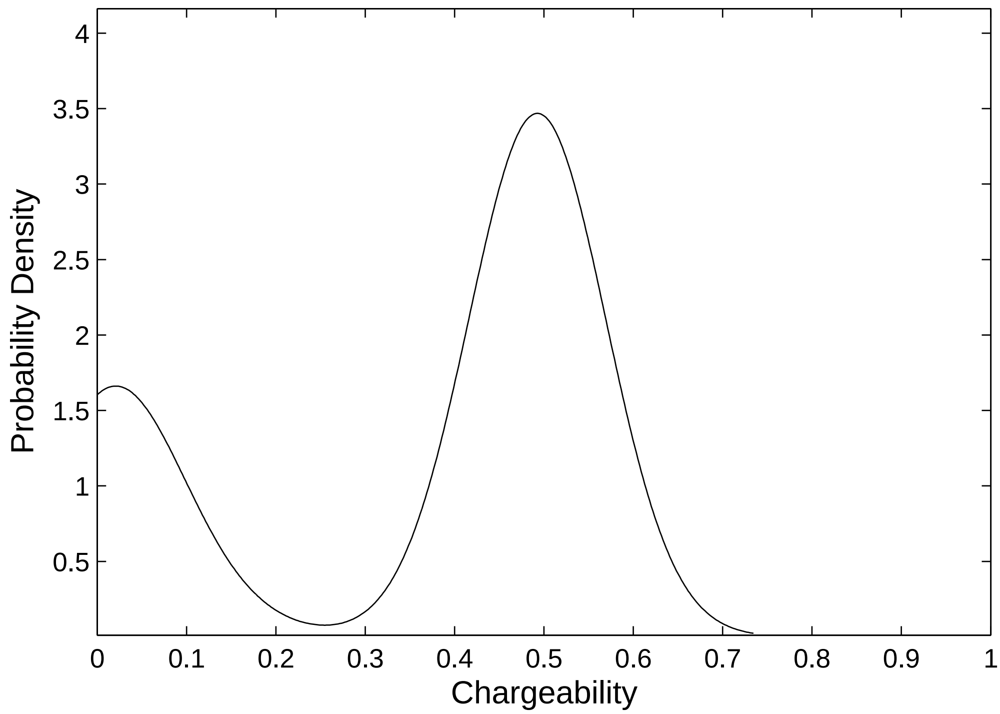

Figure 1. Estimated chargeabiliy (m_1) using the common prior ranges.

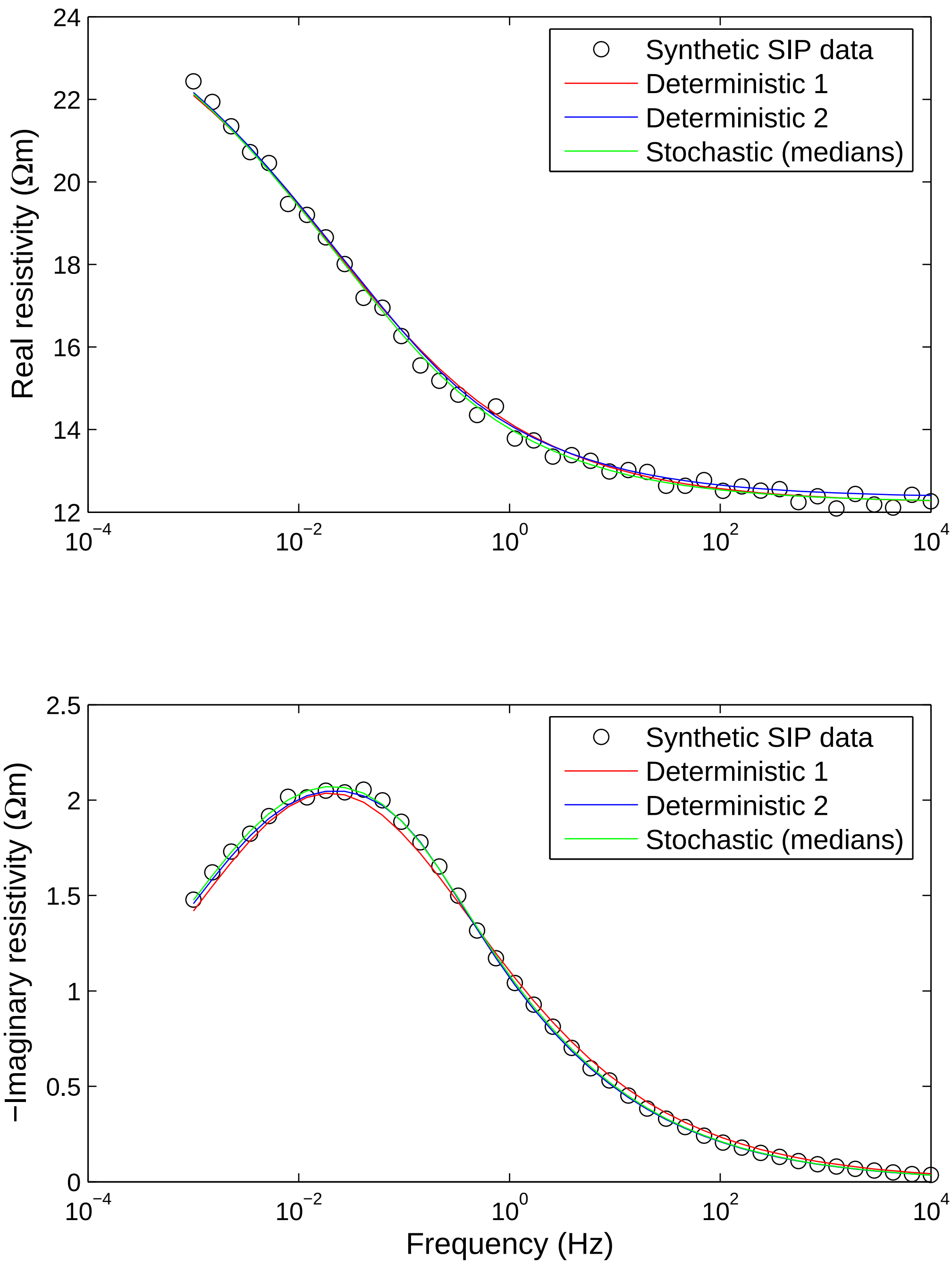

Figure 2. Synthetic SIP data with 1% relative noise and obtained fits using the stochastic method (green curves) and the deterministic method with two different sets of initial values (blue curves: true values, and red curves: Init0 values in Table 1) for a dual Cole-Cole model.

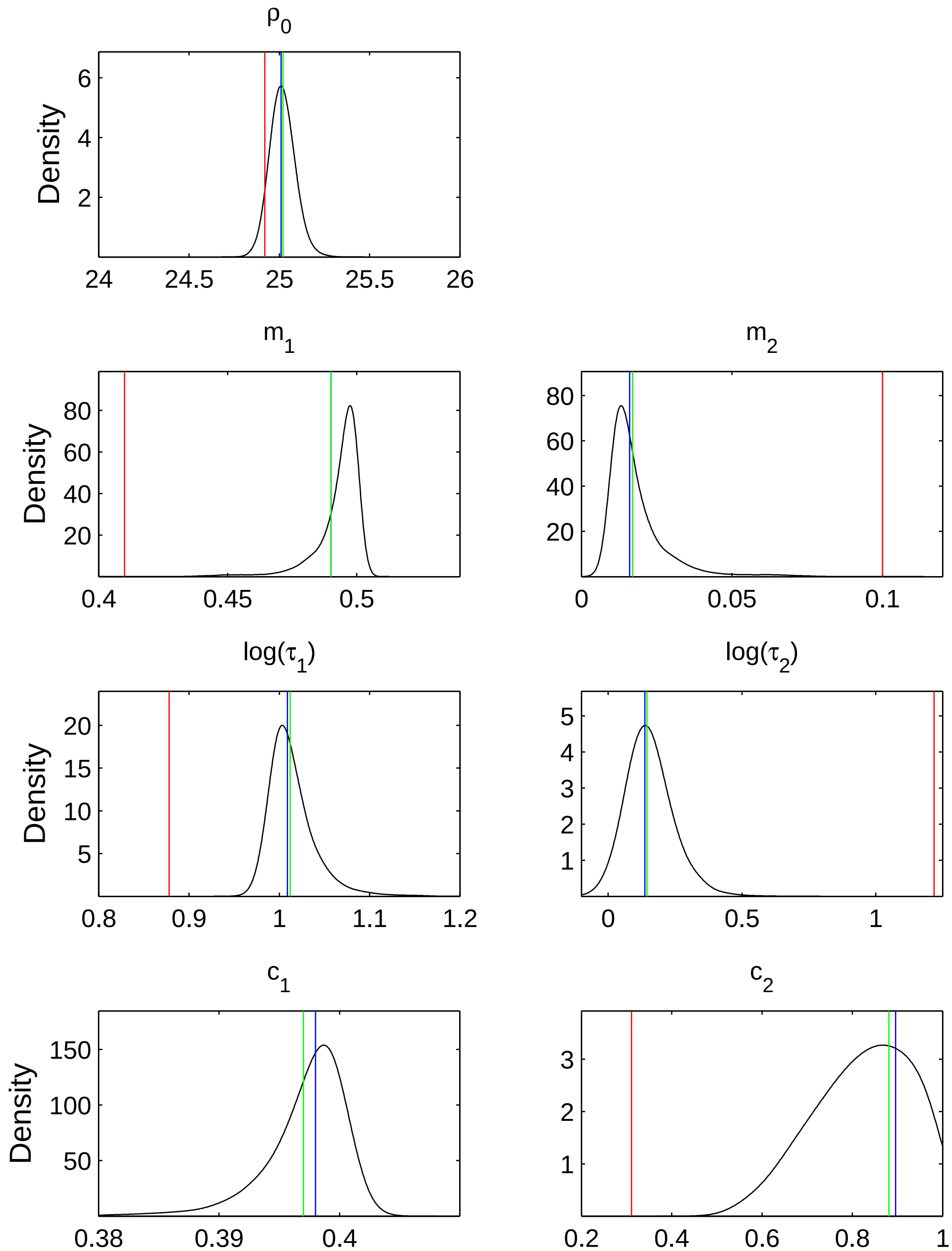

Figure 3. Comparison between the estimated pdfs from the stochastic method (black curves) and the estimated parameters from the deterministic method for three different sets of initial values (blue lines: true values, green lines: medians of the stochastic inversion results, and red lines: Init0 values in Table 1) for the synthetic SIP data with 1% relative noise using a dual Cole-Cole model.

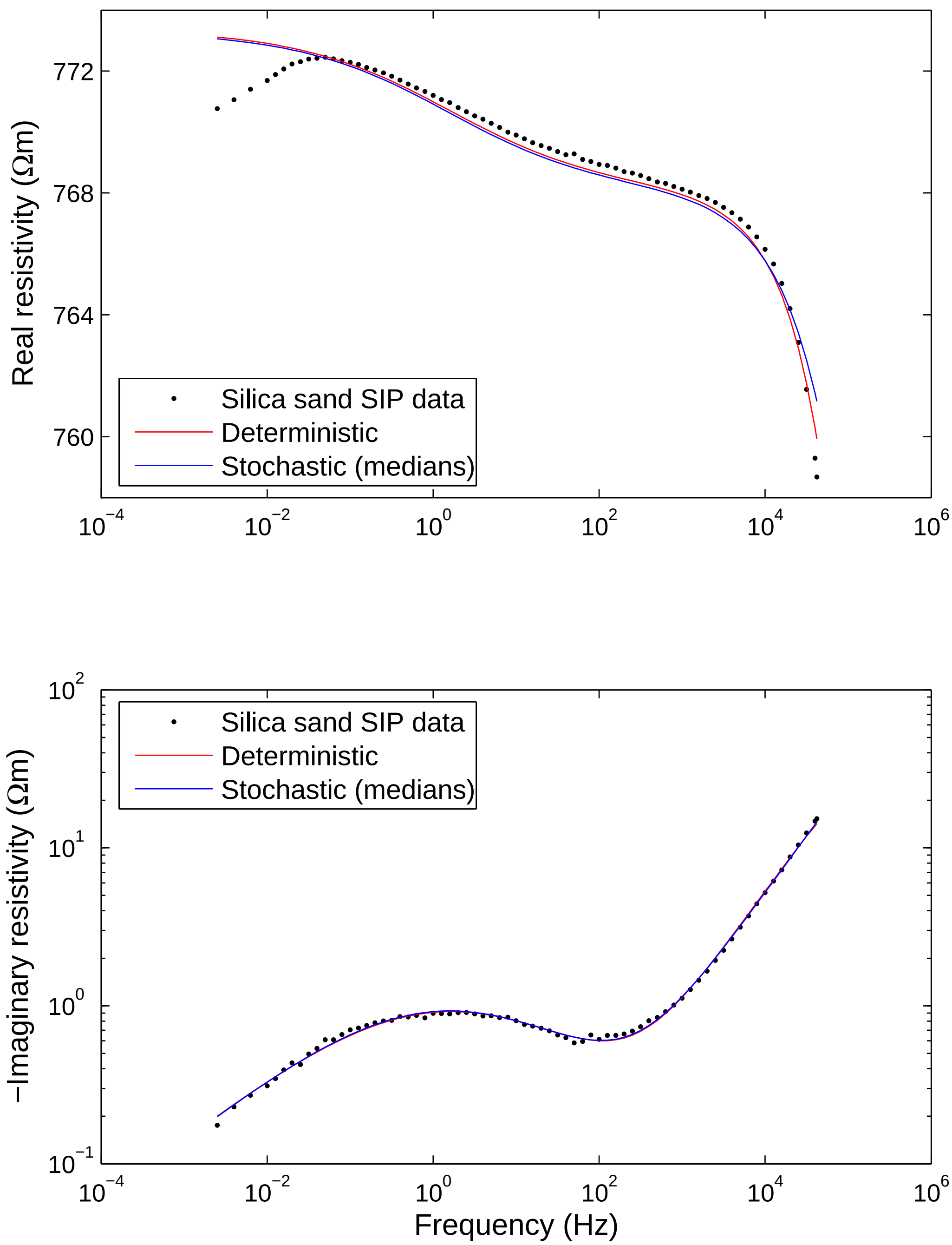

Figure 4. Silica sand SIP data and obtained fits using the stochastic (blue curves) and the deterministic (red curves) methods for a dual Cole-Cole model.

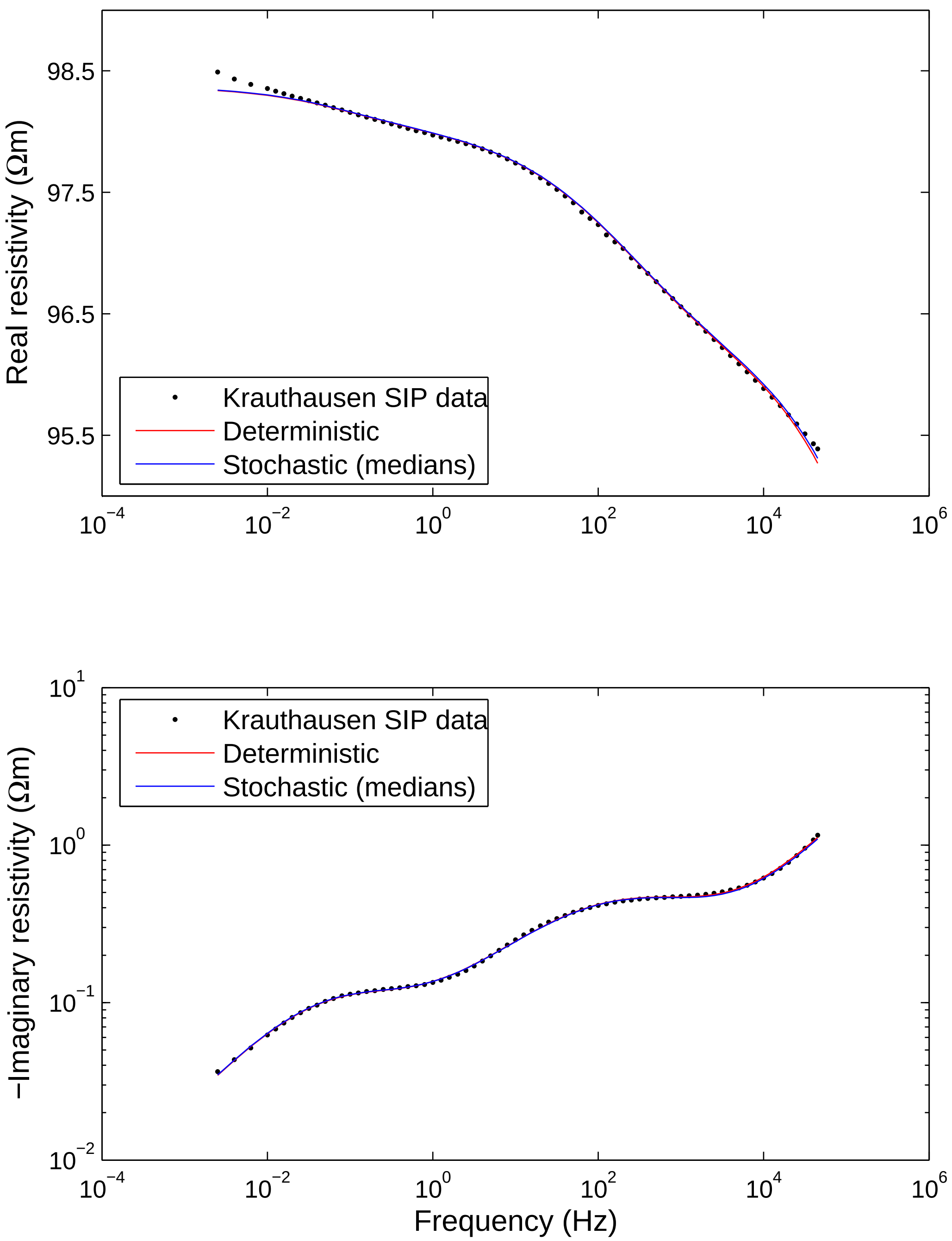

Figure 5. Krauthausen SIP data and obtained fits using the stochastic (blue curves) and the deterministic (red curves) methods for a triple Cole-Cole model.

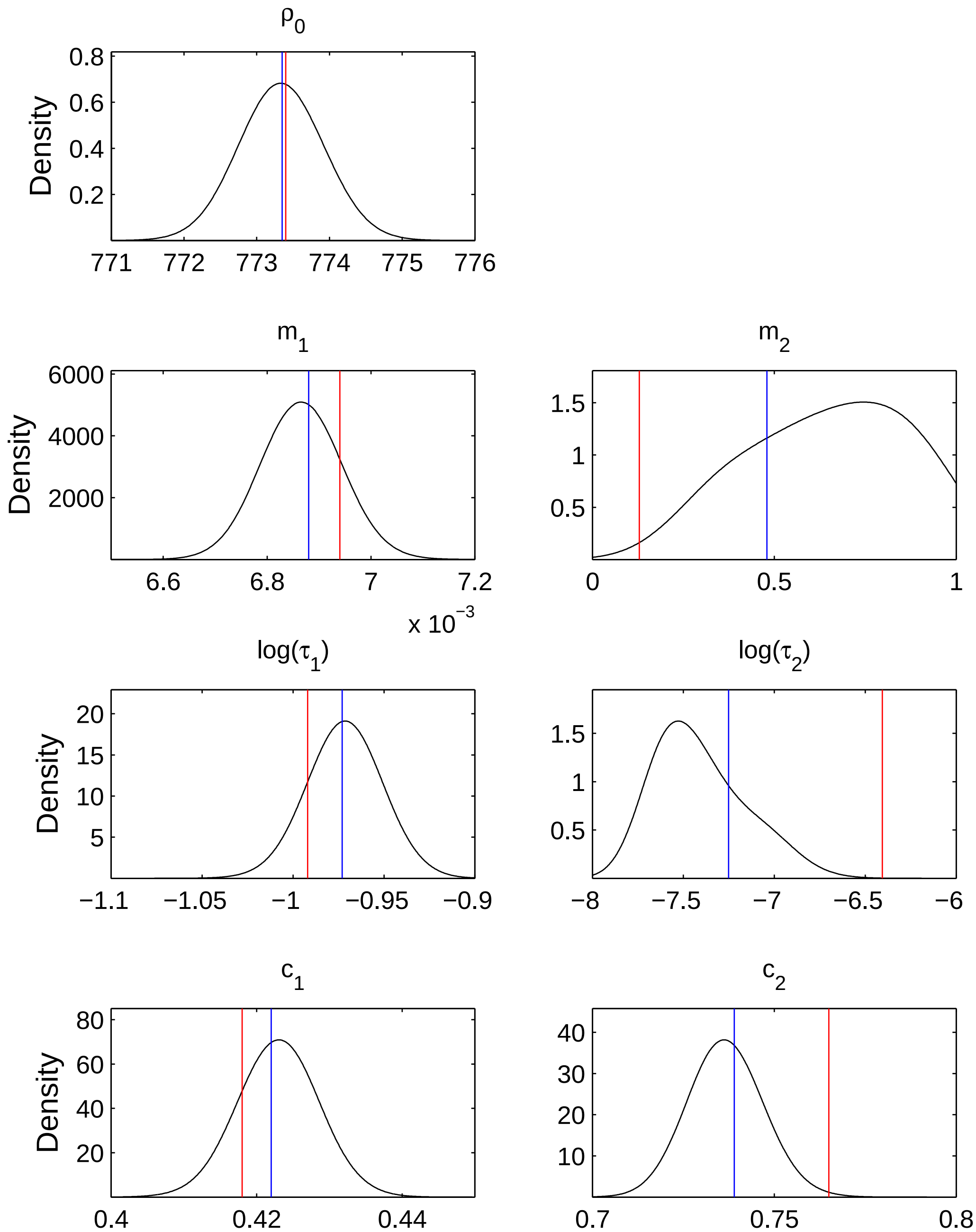

Figure 6. Comparison between the estimated pdfs from the stochastic method (black curves) and the estimated parameters from the deterministic method for two different sets of initial values (blue lines: medians of the stochastic inversion results, and red lines: values found from test tries) for the silica sand SIP data using a dual Cole-Cole model.

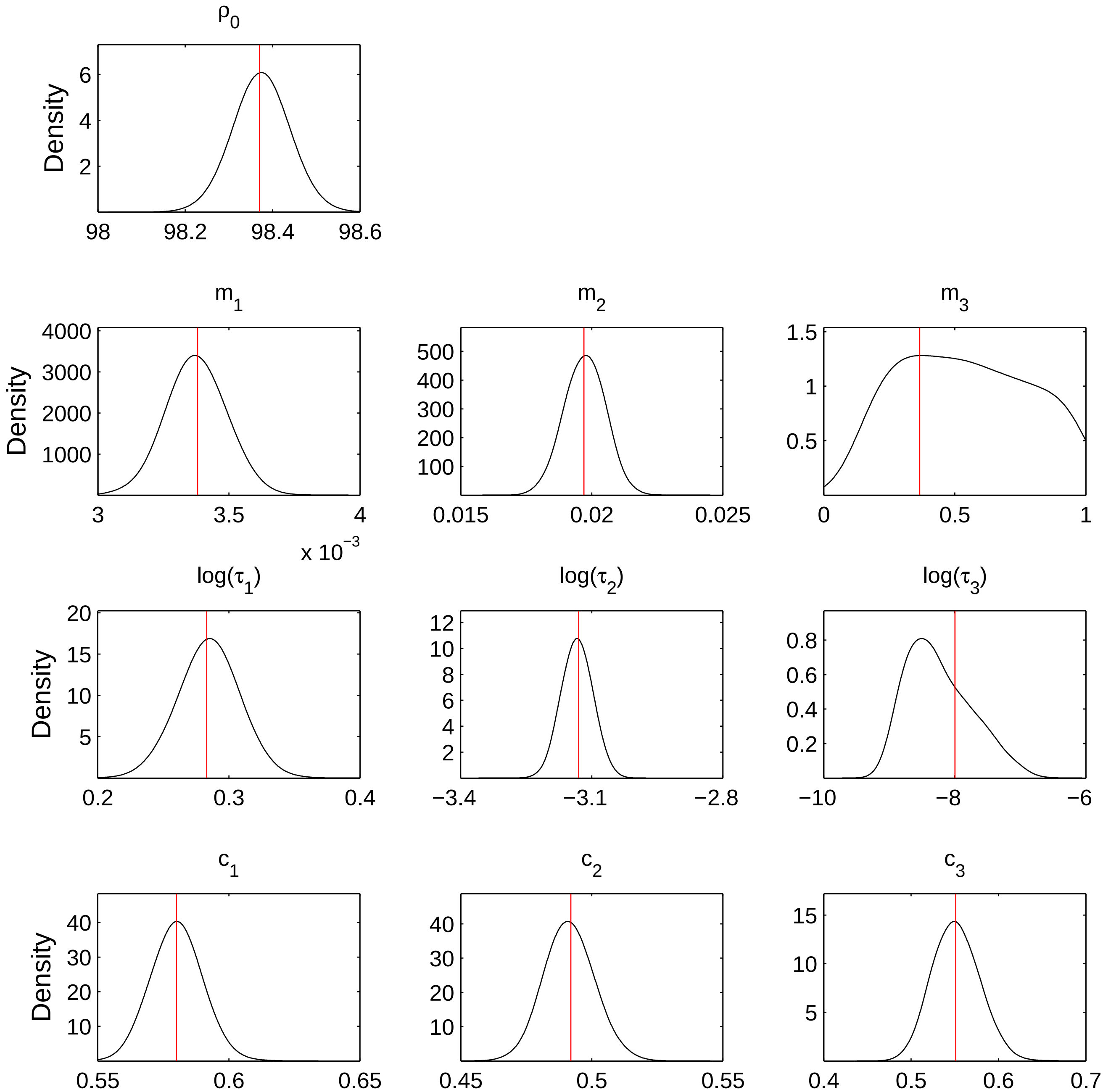

Figure 7. Comparison between the estimated pdfs from the stochatsic method (black curves) and the estimated parameters from the deterministic method (red lines) for the Krauthausen SIP data using a triple Cole-Cole model.